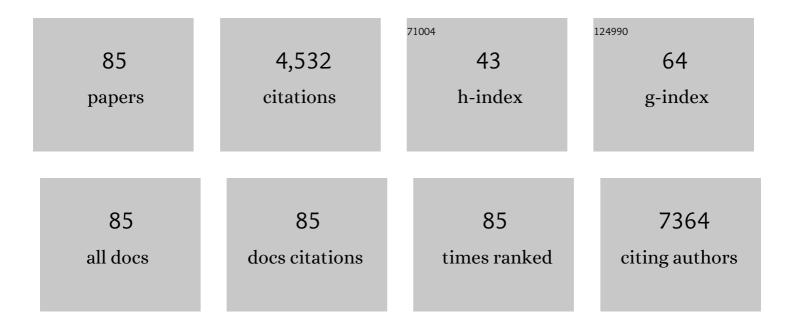
List of Publications by Year in descending order

Source: https://exaly.com/author-pdf/1238534/publications.pdf Version: 2024-02-01



#	Article	IF	CITATIONS
1	Design Strategies for Single-Atom Iron Electrocatalysts toward Efficient Oxygen Reduction. Journal of Physical Chemistry Letters, 2022, 13, 168-174.	2.1	22
2	Boosting the transport kinetics of free-standing SnS <sub>2</sub> @Carbon nanofibers by electronic structure modulation for advanced lithium storage. Journal of Materials Chemistry A, 2022, 10, 9468-9481.	5.2	9
3	Surface Engineering of Cr-Doped Cobalt Molybdate toward High-Performance Hydrogen Evolution. ACS Applied Materials & Interfaces, 2022, 14, 18607-18615.	4.0	12
4	Reconstruction-induced NiCu-based catalysts towards paired electrochemical refining. Energy and Environmental Science, 2022, 15, 3004-3014.	15.6	51
5	A Glassâ€Ceramic with Accelerated Surface Reconstruction toward the Efficient Oxygen Evolution Reaction. Angewandte Chemie - International Edition, 2021, 60, 3773-3780.	7.2	164
6	A Classâ€Ceramic with Accelerated Surface Reconstruction toward the Efficient Oxygen Evolution Reaction. Angewandte Chemie, 2021, 133, 3817-3824.	1.6	28
7	A phosphate semiconductor-induced built-in electric field boosts electron enrichment for electrocatalytic hydrogen evolution in alkaline conditions. Journal of Materials Chemistry A, 2021, 9, 13109-13114.	5.2	23
8	Incomplete amorphous phosphorization on the surface of crystalline cobalt molybdate to accelerate hydrogen evolution. Journal of Materials Chemistry A, 2021, 9, 21859-21866.	5.2	16
9	Spider Web-like Flexible Tactile Sensor for Pressure-Strain Simultaneous Detection. ACS Applied Materials & Interfaces, 2021, 13, 10428-10436.	4.0	37
10	Activating inverse spinel NiCo2O4 embedded in N-doped carbon nanofibers via Fe substitution for bifunctional oxygen electrocatalysis. Materials Today Physics, 2021, 17, 100353.	2.9	29
11	Crystallinity Effect of NiFe LDH on the Growth of Pt Nanoparticles and Hydrogen Evolution Performance. Journal of Physical Chemistry Letters, 2021, 12, 7221-7228.	2.1	16
12	Hollow MXene Sphere-Based Flexible E-Skin for Multiplex Tactile Detection. ACS Applied Materials & Interfaces, 2021, 13, 45924-45934.	4.0	34
13	Optimized electron occupancy of solid-solution transition metals for suppressing the oxygen evolution of Li <sub>2</sub> MnO <sub>3</sub> . Journal of Materials Chemistry A, 2021, 9, 9337-9346.	5.2	7
14	Hollow MoS <sub>2</sub> /Co nanopillars with boosted Li-ion diffusion rate and long-term cycling stability. Chemical Communications, 2021, 57, 11521-11524.	2.2	5
15	Edge-sited Fe-N4 atomic species improve oxygen reduction activity via boosting O2 dissociation. Applied Catalysis B: Environmental, 2020, 265, 118593.	10.8	63
16	Zirconium nitride catalysts surpass platinum for oxygen reduction. Nature Materials, 2020, 19, 282-286.	13.3	293
17	A skin-like sensor for intelligent Braille recognition. Nano Energy, 2020, 68, 104346.	8.2	87
18	Highly Localized C–N2 Sites for Efficient Oxygen Reduction. ACS Catalysis, 2020, 10, 9366-9375.	5.5	21

#	Article	IF	CITATIONS
19	Interface Engineering with Ultralow Ruthenium Loading for Efficient Water Splitting. ACS Applied Materials & Interfaces, 2020, 12, 36177-36185.	4.0	35
20	Solid-solution hexagonal Ni <sub>0.5</sub> Co <sub>0.5</sub> Se nanoflakes toward boosted oxygen evolution reaction. Chemical Communications, 2020, 56, 13113-13116.	2.2	16
21	Dual-doping of ruthenium and nickel into Co <sub>3</sub> O <sub>4</sub> for improving the oxygen evolution activity. Materials Chemistry Frontiers, 2020, 4, 1390-1396.	3.2	26
22	Multidimensional graphene structures and beyond: Unique properties, syntheses and applications. Progress in Materials Science, 2020, 113, 100665.	16.0	61
23	Ultrahigh-Sensitive Finlike Double-Sided E-Skin for Force Direction Detection. ACS Applied Materials & Interfaces, 2020, 12, 14136-14144.	4.0	44
24	<i>In situ</i> growth of free-standing perovskite hydroxide electrocatalysts for efficient overall water splitting. Journal of Materials Chemistry A, 2020, 8, 5919-5926.	5.2	21
25	KOH activation of coal-derived microporous carbons for oxygen reduction and supercapacitors. RSC Advances, 2020, 10, 15707-15714.	1.7	21
26	Geometric Structure and Electronic Polarization Synergistically Boost Hydrogen Evolution Kinetics in Alkaline Medium. Journal of Physical Chemistry Letters, 2020, 11, 3436-3442.	2.1	18
27	A bimetallic MOF@graphene oxide composite as an efficient bifunctional oxygen electrocatalyst for rechargeable Zn–air batteries. Dalton Transactions, 2020, 49, 5730-5735.	1.6	48
28	Mechanochemical synthesis of multi-site electrocatalysts as bifunctional zinc–air battery electrodes. Journal of Materials Chemistry A, 2019, 7, 19355-19363.	5.2	53
29	Increased activity of nitrogen-doped graphene-like carbon sheets modified by iron doping for oxygen reduction. Journal of Colloid and Interface Science, 2019, 536, 42-52.	5.0	32
30	A Thermally Decomposable Template Route to Synthesize Nitrogen-Doped Wrinkled Carbon Nanosheets as Highly Efficient and Stable Electrocatalysts for the Oxygen Reduction Reaction. ACS Sustainable Chemistry and Engineering, 2018, 6, 1951-1960.	3.2	19
31	KOH activation of biomass-derived nitrogen-doped carbons forÂsupercapacitor and electrocatalytic oxygen reduction. Electrochimica Acta, 2018, 261, 49-57.	2.6	345
32	Auto-optimizing Hydrogen Evolution Catalytic Activity of ReS <sub>2</sub> through Intrinsic Charge Engineering. ACS Nano, 2018, 12, 4486-4493.	7.3	111
33	Efficient N-doping of hollow core-mesoporous shelled carbon spheres via hydrothermal treatment in ammonia solution for the electrocatalytic oxygen reduction reaction. Microporous and Mesoporous Materials, 2018, 261, 88-97.	2.2	62
34	Three-dimensional interconnected nitrogen-doped mesoporous carbons as active electrode materials for application in electrocatalytic oxygen reduction and supercapacitors. Journal of Colloid and Interface Science, 2018, 527, 230-240.	5.0	56
35	In situ formation of iron-cobalt sulfides embedded in N,S-doped mesoporous carbon as efficient electrocatalysts for oxygen reduction reaction. Microporous and Mesoporous Materials, 2018, 270, 1-9.	2.2	43
36	Reactive template synthesis of nitrogen-doped graphene-like carbon nanosheets derived from hydroxypropyl methylcellulose and dicyandiamide as efficient oxygen reduction electrocatalysts. Journal of Power Sources, 2017, 345, 120-130.	4.0	30

#	Article	IF	CITATIONS
37	Nitrogen-doped hollow mesoporous carbon spheres as a highly active and stable metal-free electrocatalyst for oxygen reduction. Carbon, 2017, 114, 177-186.	5.4	122
38	Non-noble bimetallic alloy encased in nitrogen-doped nanotubes as a highly active and durable electrocatalyst for oxygen reduction reaction. Carbon, 2017, 114, 347-355.	5.4	110
39	Synthesis of Nitrogen-Doped Porous Carbon Spheres with Improved Porosity toward the Electrocatalytic Oxygen Reduction. ACS Sustainable Chemistry and Engineering, 2017, 5, 11105-11116.	3.2	61
40	Ultrafine WC nanoparticles anchored on co-encased, N-doped carbon nanotubes for efficient hydrogen evolution. Energy Storage Materials, 2017, 6, 104-111.	9.5	48
41	Ditungsten carbide nanoparticles encapsulated by ultrathin graphitic layers with excellent hydrogen-evolution electrocatalytic properties. Journal of Materials Chemistry A, 2016, 4, 8204-8210.	5.2	57
42	In situ formation of nitrogen-doped carbon nanoparticles on hollow carbon spheres as efficient oxygen reduction electrocatalysts. Nanoscale, 2016, 8, 18134-18142.	2.8	52
43	The direct growth of highly dispersed CoO nanoparticles on mesoporous carbon as a high-performance electrocatalyst for the oxygen reduction reaction. RSC Advances, 2016, 6, 70763-70769.	1.7	12
44	Self-Assembly of Nitrogen-doped Graphene-Wrapped Carbon Nanoparticles as an Efficient Electrocatalyst for Oxygen Reduction Reaction. Electrochimica Acta, 2016, 216, 347-354.	2.6	19
45	Phosphorus/sulfur Co-doped porous carbon with enhanced specific capacitance for supercapacitor and improved catalytic activity for oxygen reduction reaction. Journal of Power Sources, 2016, 314, 39-48.	4.0	141
46	Ionic liquid-assisted synthesis of dual-doped graphene as efficient electrocatalysts for oxygen reduction. Carbon, 2016, 102, 58-65.	5.4	50
47	Novel synthesis of N-doped graphene as an efficient electrocatalyst towards oxygen reduction. Nano Research, 2016, 9, 808-819.	5.8	81
48	Capacitive behaviour of MnF2 and CoF2 submicro/nanoparticles synthesized via a mild ionic liquid-assisted route. Journal of Power Sources, 2016, 303, 49-56.	4.0	29
49	An In Situ Sourceâ€Templateâ€Interface Reaction Route to 3D Nitrogenâ€Doped Hierarchical Porous Carbon as Oxygen Reduction Electrocatalyst. Advanced Materials Interfaces, 2015, 2, 1500199.	1.9	39
50	Facile synthesis of porous Li-rich layered Li[Li <sub>0.2</sub> Mn <sub>0.534</sub> Ni <sub>0.133</sub> Co <sub>0.133</sub> ]O <sub>2</sub> as high-performance cathode materials for Li-ion batteries. RSC Advances, 2015, 5, 30507-30513.	1.7	20
51	A facile nanocasting strategy to nitrogen-doped porous carbon monolith by treatment with ammonia for efficient oxygen reduction. Journal of Materials Chemistry A, 2015, 3, 12836-12844.	5.2	44
52	Spinel nickel ferrite nanoparticles strongly cross-linked with multiwalled carbon nanotubes as a bi-efficient electrocatalyst for oxygen reduction and oxygen evolution. RSC Advances, 2015, 5, 73834-73841.	1.7	58
53	Graphene/acid assisted facile synthesis of structure-tuned Fe3O4 and graphene composites as anode materials for lithium ion batteries. Carbon, 2015, 86, 310-317.	5.4	61
54	Trimetallic PtAgCu@PtCu core@shell concave nanooctahedrons with enhanced activity for formic acid oxidation reaction. Nano Energy, 2015, 12, 824-832.	8.2	126

#	Article	IF	CITATIONS
55	Polyanilineâ€Coated Hollow Fe <sub>2</sub> O <sub>3</sub> Nanoellipsoids as an Anode Material for Highâ€Performance Lithiumâ€Ion Batteries. ChemElectroChem, 2015, 2, 503-507.	1.7	22
56	In situ growth of spinel CoFe <sub>2</sub> O <sub>4</sub> nanoparticles on rod-like ordered mesoporous carbon for bifunctional electrocatalysis of both oxygen reduction and oxygen evolution. Journal of Materials Chemistry A, 2015, 3, 15598-15606.	5.2	86
57	Facile Synthesis of Hollow Mesoporous CoFe <sub>2</sub> O <sub>4</sub> Nanospheres and Graphene Composites as Highâ€Performance Anode Materials for Lithiumâ€Ion Batteries. ChemElectroChem, 2015, 2, 1010-1018.	1.7	45
58	Solvothermally synthesized graphene nanosheets supporting spinel NiFe <sub>2</sub> O <sub>4</sub> nanoparticles as an efficient electrocatalyst for the oxygen reduction reaction. RSC Advances, 2015, 5, 44476-44482.	1.7	22
59	Halideâ€Ionâ€Assisted Synthesis of Different αâ€Fe <sub>2</sub> O <sub>3</sub> Hollow Structures and Their Lithiumâ€Ion Storage Properties. ChemPlusChem, 2015, 80, 522-528.	1.3	14
60	Synthesis of carbon nanotube/mesoporous TiO2 coaxial nanocables with enhanced lithium ion battery performance. Carbon, 2014, 75, 345-352.	5.4	44
61	Polymer-pyrolysis assisted synthesis of vanadium trioxide and carbon nanocomposites as high performance anode materials for lithium-ion batteries. Journal of Power Sources, 2014, 261, 184-187.	4.0	52
62	Hydrothermal synthesis of Pt–Ag alloy nano-octahedra and their enhanced electrocatalytic activity for the methanol oxidation reaction. Nanoscale, 2014, 6, 12310-12314.	2.8	56
63	One-pot scalable synthesis of Cu–CuFe <sub>2</sub> O <sub>4</sub> /graphene composites as anode materials for lithium-ion batteries with enhanced lithium storage properties. Journal of Materials Chemistry A, 2014, 2, 13892.	5.2	56
64	Facile synthesis of CuO nanoneedle electrodes for high-performance lithium-ion batteries. Materials Chemistry and Physics, 2014, 148, 411-415.	2.0	22
65	Scalable synthesis of Fe3O4 nanoparticles anchored on graphene as a high-performance anode for lithium ion batteries. Journal of Solid State Chemistry, 2013, 201, 330-337.	1.4	43
66	Layered Li2MnO3·3LiNi0.5â^'xMn0.5â^'xCo2xO2 microspheres with Mn-rich cores as high performance cathode materials for lithium ion batteries. Physical Chemistry Chemical Physics, 2013, 15, 16579.	1.3	17
67	A three-dimensional graphene scaffold supported thin film silicon anode for lithium-ion batteries. Journal of Materials Chemistry A, 2013, 1, 10092.	5.2	88
68	Solvothermal Synthesis of Monodisperse LiFePO <sub>4</sub> Micro Hollow Spheres as High Performance Cathode Material for Lithium Ion Batteries. ACS Applied Materials & Interfaces, 2013, 5, 8961-8967.	4.0	62
69	Force induced phase transition of honeycomb-structured ferroelectric thin film. Physica A: Statistical Mechanics and Its Applications, 2013, 392, 3570-3577.	1.2	13
70	Fabrication of FeF3 nanocrystals dispersed into a porous carbon matrix as a high performance cathode material for lithium ion batteries. Journal of Materials Chemistry A, 2013, 1, 15060.	5.2	72
71	Fabrication of LiF/Fe/Graphene Nanocomposites As Cathode Material for Lithium-Ion Batteries. ACS Applied Materials & Interfaces, 2013, 5, 892-897.	4.0	50
72	Thermal evaporation-induced anhydrous synthesis of Fe3O4–graphene composite with enhanced rate performance and cyclic stability for lithium ion batteries. Physical Chemistry Chemical Physics, 2013, 15, 7174.	1.3	58

#	Article	IF	CITATIONS
73	Single-crystalline Li4Ti5O12 nanorods and their application in high rate capability Li4Ti5O12/LiMn2O4 full cells. Journal of Power Sources, 2013, 242, 222-229.	4.0	34
74	Evaporation-induced synthesis of carbon-supported Fe3O4 nanocomposites as anode material for lithium-ion batteries. CrystEngComm, 2013, 15, 1324.	1.3	38
75	Large-scale fabrication of graphene-wrapped FeF3 nanocrystals as cathode materials for lithium ion batteries. Nanoscale, 2013, 5, 6338.	2.8	77
76	Triethylene Glycol Assisted Synthesis of Pure Tavorite LiFeSO <sub>4</sub> F Cathode Material for Li-Ion Battery. Journal of the Electrochemical Society, 2013, 160, A3072-A3076.	1.3	12
77	Large-scale fabrication of hierarchical α-Fe2O3 assemblies as high performance anode materials for lithium-ion batteries. CrystEngComm, 2012, 14, 7882.	1.3	16
78	Facile synthesis and electrochemical characterization of Sn4Ni3/C nanocomposites as anode materials for lithium ion batteries. Journal of Solid State Chemistry, 2012, 196, 536-542.	1.4	17
79	Rugated porous Fe3O4 thin films as stable binder-free anode materials for lithium ion batteries. Journal of Materials Chemistry, 2012, 22, 22692.	6.7	30
80	Solvothermal synthesis of nano-LiMnPO4 from Li3PO4 rod-like precursor: reaction mechanism and electrochemical properties. Journal of Materials Chemistry, 2012, 22, 25402.	6.7	51
81	Facile and Rapid Synthesis of Highly Porous Wirelike TiO <sub>2</sub> as Anodes for Lithium-Ion Batteries. ACS Applied Materials & Interfaces, 2012, 4, 1608-1613.	4.0	57
82	Growth of TiO2 nanorod arrays on reduced graphene oxide with enhanced lithium-ion storage. Journal of Materials Chemistry, 2012, 22, 19061.	6.7	65
83	Facile synthesis of porous LiMn2O4 spheres as positive electrode for high-power lithium ion batteries. Journal of Power Sources, 2012, 198, 251-257.	4.0	122
84	Microwave-assisted hydrothermal synthesis of porous SnO2 nanotubes and their lithium ion storage properties. Journal of Solid State Chemistry, 2012, 190, 104-110.	1.4	46
85	Synthesis and properties of nanostructured dense LaB6 cathodes by arc plasma and reactive spark plasma sintering. Acta Materialia, 2010, 58, 4978-4985.	3.8	57